PHYSICAL REVIEW D **71,** 014032 (2005)

Volume dependence of the pion mass in the quark-meson model

J. Braun,[1] B. Klein,[1] and H. J. Pirner[1,2]

[1]*Institute for Theoretical Physics, University of Heidelberg, Philosophenweg 19, 69120 Heidelberg, Germany*
[2]*Max-Planck-Institut für Kernphysik, Saupfercheckweg 1, 69117 Heidelberg, Germany*

(Received 13 August 2004; published 26 January 2005)

We consider the quark-meson-model in a finite three-dimensional volume using the Schwinger proper-time renormalization group. We derive and solve the flow equations for finite volume in local potential approximation. In order to break chiral symmetry in the finite volume, we introduce a small current quark mass. The corresponding effective meson potential breaks chiral O(4) symmetry explicitly, depending on σ and $\vec{\pi}$ fields separately. We calculate the volume dependence of the pion mass and of the pion decay constant with the renormalization group flow equations and compare with recent results from chiral perturbation theory in a finite volume.

DOI: 10.1103/PhysRevD.71.014032 PACS numbers: 12.38.Lg, 12.39.Fe

I. INTRODUCTION

The study of QCD in a finite volume has been of interest for quite some time. Accurate results of lattice simulations with dynamical fermions necessitate understanding finite volume effects. A variety of different methods has been proposed cf. refs. [1–9], to extrapolate reliably from finite lattice volumes to the infinite volume. Finite volume partition functions for QCD have attracted interest in their own right, because they allow an exact description of QCD at low energies [10–13]. The low-energy behavior of QCD is determined by spontaneous chiral symmetry breaking [14], which, however, does not occur in a finite volume. If the current quark mass is set equal to zero, in a finite volume the expectation value for the order parameter of chiral symmetry breaking vanishes, remaining zero even for arbitrary large volumes. The order parameter has a finite expectation value only when the infinite volume limit is taken before the quark mass is set to zero.

The box size L, the pion mass m_π, and the pion decay constant f_π are the relevant scales for the transition between the regimes with a strongly broken and an effectively restored chiral symmetry [10]. As a measure of explicit symmetry breaking, the pion mass is of particular importance. It is primarily the dimensionless product $m_\pi L$ that determines in which regime the system exists for a given pion mass and volume. In order to study chiral symmetry breaking in a finite volume, it is essential to introduce a finite quark mass as a parameter that explicitly breaks the chiral symmetry. Such an explicit symmetry breaking is quite natural in theories which involve effective chiral Lagrangians.

QCD at low energy can be studied by a wide variety of approaches which in essence all rely on the same fact: Because of spontaneous breaking of chiral symmetry, low-energy QCD is dominated by massless Goldstone bosons associated with the broken symmetry. Since these Goldstone bosons interact only weakly, the low-energy limit of QCD can be described in terms of an effective theory of these fields. A description in terms of effective chiral Lagrangians becomes even better if one considers the partition functions in finite Euclidean volume. Compared to the light degrees of freedom, contributions of heavier particles are suppressed by e^{-ML}, where M is the typical separation of the hadronic mass scale from the Goldstone masses. This separation of mass scales is at the origin of the description of QCD with effective theories in terms of the light degrees of freedom only.

Groundbreaking work has been done by Gasser and Leutwyler [10–12] in chiral perturbation theory, and by Leutwyler and Smilga for the eigenvalue spectrum of the QCD Dirac operator [13]. Random matrix theory [15,16] predicts analytically the volume and quark mass dependence of the chiral condensate [17–19], and the eigenvalue spectrum which has been well confirmed by numerous lattice results, see eg., [19–21]. Such analytic predictions have been extremely useful as a check for calculations in lattice gauge theory.

In the context of the renormalization group (RG) approach, most calculations so far have been done in a chirally symmetric formulation [22–25]. In such a framework, explicit symmetry-breaking terms do not affect the renormalization group flow. This means that pion contributions to the renormalization group flow come from exactly massless pions. Small quark masses can be converted into a small linear term in the meson potential which is not renormalized and can therefore be added at the end of the evolution. In this paper, we will present a formulation which includes explicit symmetry breaking in the renormalization group flow and which can be used also for a finite volume.

We use the chiral quark-meson model, which contains a scalar sigma meson and quarks in addition to the pion degrees of freedom. It is well known that the linear sigma model alone is not compatible with the low-energy $\pi\pi$-scattering data [14]. Because of the presence of quarks, the low-energy constants of chiral perturbation theory are reproduced [26,27]. The quark-meson model is evolved with renormalization group flow equations

which connect different scales. As we will demonstrate, the inverse box size $1/L$ acts as an effective cutoff scale which freezes the evolution when the evolution parameter $k < \pi/L$. In the same way as the renormalization group flow equations describe the dependence of the results on the renormalization cutoff scale k, they also describe the dependence on the additional scale imposed by the finite volume. The summation of higher loop graphs in this approach does allow to extend the calculation to smaller quark masses and volumes, where perturbative calculations lack convergence. Deviations of the calculated pion mass correction in the finite volume from chiral perturbation theory are found in this region. Our results agree, however, in the case of large pion masses and large volumes.

The paper is organized as follows: In section II, we review recent results from the application of chiral perturbation theory to the problem of finite volume effects. In section III, we show how the evolution equation for the effective meson potential is modified in a finite volume. Details of the numerical evaluation are discussed in section IV. In section V we present our final results, which are discussed in section VI.

II. FINITE VOLUME EFFECTS IN CHIRAL PERTURBATION THEORY

For finite volume, massless Goldstone bosons dominate the action of a theory with broken chiral symmetry. In chiral perturbation theory (chPT) [14], the pion mass, the pion decay constant, and the chiral condensate have been calculated [10–12]. The expansion parameters are the magnitude of the three-momentum $|\vec{p}|$ and the mass of the pion m_π as the lightest degree of freedom compared with the chiral symmetry-breaking scale $4\pi f_\pi$.

Depending on the size L of the volume and the pion mass m_π, chiral perturbation theory distinguishes between two different power counting schemes. If the size of the box is much larger than the Compton wavelength of the pion $L \gg 1/m_\pi$, the lowest nonzero pion momentum is smaller than the pion mass ($p_{\min} \sim \frac{2\pi}{L} \ll m_\pi$) and the normal power counting scheme applies (''p-regime''). In this case, the pions are constrained very little by the presence of the box, and finite size effects are comparatively small [12]. If, on the other hand, the size of the box is smaller than the Compton wavelength of the pion, the normal chiral expansion breaks down, since the smallest momentum $p_{\min} \sim \frac{2\pi}{L} \gg m_\pi$ is now much larger than the pion mass (''ϵ-regime''). In this case, the partition function is dominated by the zero modes. After solving the zero-momentum sector of the theory exactly, one expands the finite momentum modes to one-loop order.

A very useful tool to study the effects of a finite volume on the mass of the pion is Lüscher's formula [28]. It relates the leading finite volume corrections for the pion mass in Euclidean volume to the $\pi\pi$-scattering amplitude in infinite volume. Corrections to the leading order behavior drop at the least as $\mathcal{O}(e^{-\bar{m}L})$ where $\bar{m} \geq \sqrt{3/2}m_\pi$. For the particular case of the pion mass, the formula for the relative deviation $R[m_\pi(L)]$ of the pion mass $m_\pi(L)$ in the finite volume from the pion mass in the infinite volume $m_\pi(\infty)$ reads as follows:

$$\begin{aligned} R[m_\pi(L)] &= \frac{m_\pi(L) - m_\pi(\infty)}{m_\pi(\infty)} \\ &= -\frac{3}{16\pi^2}\frac{1}{m_\pi}\frac{1}{m_\pi L}\int_{-\infty}^{\infty} dy F(iy) e^{-\sqrt{m_\pi^2+y^2}L} \\ &\quad + \mathcal{O}(e^{-\bar{m}L}). \end{aligned} \tag{1}$$

F is the forward $\pi\pi$-scattering amplitude as a function of the energy variable s continued to complex values. New results [8,9] have recently been obtained by combining Lüscher's formula with a calculation of the scattering amplitude in chiral perturbation theory. A next-to-next-to leading order calculation of F alone does not seem to give a reliable and satisfactory result. A one-loop calculation using Lüscher's formula gives a shift in the pion mass, for example, which is substantially lower than the one expected form the full one-loop calculation in chiral perturbation theory as performed by Gasser and Leutwyler [11]. This estimate of the finite volume effects can be improved, if one uses the mass correction obtained from Lüscher's formula with a $\pi\pi$-scattering amplitude including higher orders to correct the full one-loop chiral perturbation theory result [9]. Since Lüscher's formula has subleading corrections $\mathcal{O}(\exp[-\sqrt{3/2}m_\pi L])$, the corrections to the leading result increase for decreasing pion mass at fixed volume size L with $m_\pi L$. As pointed out by the authors in [9], the Lüscher formula becomes a less reliable approximation exactly for those values of the pion mass for which the chiral expansion converges especially well.

The renormalization group flow equations do not rely on either box size or pion mass as an expansion parameter, and do not require to distinguish between two different regimes. They remain valid as long as the lowest momenta and the masses of the heaviest particles remain below the ultraviolet cutoff scale $\Lambda_{UV} \approx 1.5$ GeV. The beauty of the renormalization group method is precisely that the flow equations connect different scales. In the same way as the renormalization group flow equations describe the dependence of the results on the infrared cutoff scale k, they also describe the dependence on the additional scale imposed by the finite volume.

III. RENORMALIZATION GROUP FLOW EQUATIONS FOR THE QUARK-MESON MODEL

The quark-meson model is an $\mathrm{SU}(2)_L \otimes \mathrm{SU}(2)_R$ invariant linear σ-model with chiral mesons $\phi = (\sigma, \vec{\pi})$ coupled to constituent quarks q. It is an effective model for dynamical spontaneous chiral symmetry breaking at intermediate scales of $k \lesssim \Lambda_{UV}$, where the ultraviolet scale $\Lambda_{UV} \approx 1.5$ GeV is determined by the validity of a had-

ronic representation of QCD. At the UV scale Λ_{UV}, the quark-meson model is defined by the effective action

$$\Gamma_{\Lambda_{UV}}[\phi] = \int d^4x\{\bar{q}\gamma\partial q + g\bar{q}(\sigma + i\vec{\tau}\cdot\vec{\pi}\gamma_5)q + \frac{1}{2}(\partial_\mu\phi)^2 + U(\phi) + m_c\bar{q}q\} \quad (2)$$

in a four-dimensional Euclidean volume with compact Euclidean time direction. The partition function Z has the path integral representation

$$Z = \int \mathcal{D}\bar{q}\int \mathcal{D}q\int \mathcal{D}\phi\exp(-\Gamma_{\Lambda_{UV}}), \quad (3)$$

where in the Euclidean time direction periodic and antiperiodic boundary conditions apply for bosons and fermions, respectively. A Gaussian approximation to the path integral followed by a Legendre transformation yields the one-loop effective action for the scalar fields ϕ,

$$\Gamma[\phi] = \Gamma_{\Lambda_{UV}}[\phi] - \mathrm{Tr}\log(\Gamma_F^{(2)}[\phi]) + \frac{1}{2}\mathrm{Tr}\log(\Gamma_B^{(2)}[\phi]), \quad (4)$$

where $\Gamma_B^{(2)}[\phi]$ and $\Gamma_F^{(2)}[\phi]$ are the inverse two-point functions for the bosonic and fermionic fields, evaluated at the vacuum expectation value of the mesonic field ϕ. Here, the boundary conditions of the functional integral appear in the momentum traces and we neglect contributions from mixed quark-meson-loops. In order to regularize the functional traces, we use the Schwinger proper time representation of the logarithms. We consider the effective action Γ in a local potential approximation (LPA), which represents the lowest order in the derivative expansion and incorporates fermionic as well as bosonic contributions to the potential density U. In this approximation, the effective field ϕ is considered to be constant over the entire volume.

The scale dependence is introduced through the infrared cutoff function $f_a(\tau k^2)$, which regularizes the Schwinger proper time integral. A cutoff function of the form

$$k\frac{\partial}{\partial k}f_a(\tau k^2) = -\frac{2}{\Gamma(a+1)}(\tau k^2)^{a+1}e^{-\tau k^2} \quad (5)$$

satisfies the required regularization conditions [22–24,29]. We obtain a renormalization group flow equation for the effective potential by performing a renormalization group improvement and replacing the bare two-point functions by the renormalized, scale-dependent two-point functions,

$$k\frac{\partial}{\partial k}\Gamma_k[\phi] = \frac{1}{2}\mathrm{Tr}\int_0^\infty\frac{d\tau}{\tau}\left[k\frac{\partial}{\partial k}f_a(\tau k^2)\right]\exp(-\tau\Gamma_{B,k}^{(2)}[\phi]) - \mathrm{Tr}\int_0^\infty\frac{d\tau}{\tau}\left[k\frac{\partial}{\partial k}f_a(\tau k^2)\right]\exp(-\tau\Gamma_{F,k}^{(2)}[\phi]). \quad (6)$$

In LPA, the effective action reduces to the effective potential by the relation

$$\Gamma_k[\phi] = \int d^4x U_k(\phi). \quad (7)$$

The renormalization group improved evolution equation for the effective potential in infinite volume is given by

$$k\frac{\partial}{\partial k}U_k(\phi, L\to\infty, T) = \frac{1}{2}\int_0^\infty\frac{d\tau}{\tau}\int\frac{d^4p}{(2\pi)^4}\times\{4N_cN_f\exp(-\tau[p^2 + M_q^2(\sigma,\vec{\pi}^2)]) - \exp(-\tau[p^2 + M_\sigma^2(\phi^2)]) - 3\exp(-\tau[p^2 + M_\pi^2(\phi^2)])\}k\frac{\partial}{\partial k}f_a(\tau k^2). \quad (8)$$

It is necessary to choose the parameter a in such a way that the resulting integrals over the proper time parameter τ remain finite. In infinite volume, the lowest possible integer value is $a = 2$. The diagonalization of the meson mass matrix gives the running meson masses which depend on the effective potential. Without explicit symmetry breaking, they are of the form

$$M_\sigma^2 = 2\frac{\partial U_k}{\partial\phi^2} + 4\phi^2\frac{\partial^2U_k}{(\partial\phi^2)^2}, \quad (9)$$

$$M_\pi^2 = 2\frac{\partial U_k}{\partial\phi^2}. \quad (10)$$

To derive renormalization group flow equations in the finite volume L^{d-1} at finite temperature T, we replace the integrals over the momenta by a sum

$$\int dp_i\ldots\to\frac{2\pi}{L}\sum_{n=-\infty}^{\infty}\ldots \quad (11)$$

and apply periodic boundary conditions for bosons and antiperiodic boundary conditions for fermions in time and spacelike directions. The sums run from $-\infty$ to $+\infty$, where the vector $\vec{n}$ denotes $(n_1, n_2, ..., n_{d-1})$. The Matsubara frequencies take the value $\omega_n = 2\pi nT$ for bosons and $\nu_n = (2n+1)\pi T$ for fermions, respectively. In the following we use the short-hand notation

$$p_F^2 = \sum_{i=1}^{d-1}p_i^2 = \frac{4\pi^2}{L^2}\sum_{i=1}^{d-1}\left(n_i + \frac{1}{2}\right)^2, \quad (12)$$

$$p_B^2 = \sum_{i=1}^{d-1}p_i^2 = \frac{4\pi^2}{L^2}\sum_{i=1}^{d-1}n_i^2, \quad (13)$$

for the momenta of the fermions and bosons, respectively. In finite volume, we allow explicit symmetry breaking in the effective potential, which then becomes a function of two variables σ and $\vec{\pi}^2$ separately. The corresponding expression to Eq. (8) is

$$k\frac{\partial}{\partial k}U_k(\sigma,\vec{\pi}^2,L,T)=\frac{1}{2}\frac{T}{L^{d-1}}\int\frac{d\tau}{\tau}\times\sum_l\sum_{\vec{n}}\{4N_cN_f\exp(-\tau[\nu_l^2+p_F^2+M_q^2(\sigma,\vec{\pi}^2)])-\sum_{i=1}^{4}\exp(-\tau[\omega_l^2+p_B^2+M_i^2(\sigma,\vec{\pi}^2)])\}k\frac{\partial}{\partial k}f_a(\tau k^2). \tag{14}$$

The M_i^2, $i=1,\ldots,N_f^2$ are the eigenvalues of the second derivative matrix

$$[U_k(\sigma,\vec{\pi}^2)]^{ij}=\frac{\partial^2U_k}{\partial\phi_i\partial\phi_j} \tag{15}$$

of the meson potential $U_k(\sigma,\vec{\pi}^2)$ with respect to the fields $\phi=(\sigma,\vec{\pi})$. They depend only on the magnitude of the pion fields $\vec{\pi}^2$ and are independent of the direction. We wish to stress the importance of this point, since otherwise the meson contributions from the flow equations are not compatible with the ansatz for the potential which we will introduce below.

The second derivative matrix is given by

$$\begin{pmatrix} U_{\sigma\sigma} & U_{\vec{\pi}^2\sigma}2\pi^{(1)} & U_{\vec{\pi}^2\sigma}2\pi^{(2)} & U_{\vec{\pi}^2\sigma}2\pi^{(3)}\\ U_{\sigma\vec{\pi}^2}2\pi^{(1)} & 2U_{\vec{\pi}^2}+U_{\vec{\pi}^2\vec{\pi}^2}4(\pi^{(1)})^2 & U_{\vec{\pi}^2\vec{\pi}^2}4\pi^{(1)}\pi^{(2)} & U_{\vec{\pi}^2\vec{\pi}^2}4\pi^{(1)}\pi^{(3)}\\ U_{\sigma\vec{\pi}^2}2\pi^{(2)} & U_{\vec{\pi}^2\vec{\pi}^2}4\pi^{(2)}\pi^{(1)} & 2U_{\vec{\pi}^2}+U_{\vec{\pi}^2\vec{\pi}^2}4(\pi^{(2)})^2 & U_{\vec{\pi}^2\vec{\pi}^2}4\pi^{(2)}\pi^{(3)}\\ U_{\sigma\vec{\pi}^2}2\pi^{(3)} & U_{\vec{\pi}^2\vec{\pi}^2}4\pi^{(3)}\pi^{(1)} & U_{\vec{\pi}^2\vec{\pi}^2}4\pi^{(3)}\pi^{(2)} & 2U_{\vec{\pi}^2}+U_{\vec{\pi}^2\vec{\pi}^2}4(\pi^{(3)})^2 \end{pmatrix}, \tag{16}$$

where we have suppressed the scale index k of the potential and use the abbreviations

$$\begin{aligned} U_\sigma&=\frac{\partial U}{\partial\sigma},\\ U_{\pi^{(a)}}&=\frac{\partial U}{\partial\vec{\pi}^2}\frac{\partial\vec{\pi}^2}{\partial\pi^{(a)}}=U_{\vec{\pi}^2}2\pi^{(a)},\\ U_{\vec{\pi}^2}&=\frac{\partial U}{\partial\vec{\pi}^2}, \end{aligned} \tag{17}$$

and the corresponding expressions for the higher derivatives. The eigenvalues of this matrix are given by

$$\begin{aligned} M_1^2&=\frac{1}{2}\Big[2U_{\vec{\pi}^2}+4\vec{\pi}^2U_{\vec{\pi}^2\vec{\pi}^2}+U_{\sigma\sigma}+\sqrt{(2U_{\vec{\pi}^2}+4\vec{\pi}^2U_{\vec{\pi}^2\vec{\pi}^2}-U_{\sigma\sigma})^2+16\vec{\pi}^2U_{\sigma\vec{\pi}^2}^2}\Big],\\ M_2^2&=2U_{\vec{\pi}^2},\qquad M_3^2=2U_{\vec{\pi}^2},\\ M_4^2&=\frac{1}{2}\Big[2U_{\vec{\pi}^2}+4\vec{\pi}^2U_{\vec{\pi}^2\vec{\pi}^2}+U_{\sigma\sigma}-\sqrt{(2U_{\vec{\pi}^2}+4\vec{\pi}^2U_{\vec{\pi}^2\vec{\pi}^2}-U_{\sigma\sigma})^2+16\vec{\pi}^2U_{\sigma\vec{\pi}^2}^2}\Big]. \end{aligned} \tag{18}$$

For vanishing cross terms $U_{\sigma\vec{\pi}^2}$, the last eigenvalue reduces to $2U_{\vec{\pi}^2}+4\vec{\pi}^2U_{\vec{\pi}^2\vec{\pi}^2}$, which corresponds to a derivative in ''radial'' direction in the pion-subspace. Especially for $\vec{\pi}^2=0$, the three pion modes have equal masses. We also note that the pion fields appear only in the combination $\vec{\pi}^2$ in the eigenvalues, despite the fact that the derivative matrix contains terms linear in $\pi^{(a)}$. The reason is that the rotational symmetry of the pion space remains unbroken even in the presence of explicit symmetry-breaking terms in the sigma direction.

As discussed in [30], we are able to perform the sum over the thermal Matsubara frequencies analytically and obtain an evolution equation which contains the Fermi-Dirac-distribution $n_F(E)$ and the Bose-Einstein-distribution $n_B(E)$,

$$k\frac{\partial}{\partial k}U_k(\sigma,\vec{\pi}^2,L,T)=\frac{(-1)^a}{2\Gamma(a+1)}\frac{k^{2(a+1)}}{L^{d-1}}\frac{\partial^a}{(\partial k^2)^a}\times\sum_{\vec{n}}\Big\{\sum_{i=1}^{4}\frac{1}{E_i}[1+2n_B(E_i)]-\frac{4N_cN_f}{E_q}[1-2n_F(E_q)]\Big\}, \tag{19}$$

with

$$n_F(E)=\frac{1}{e^{E/T}+1},\qquad n_B(E)=\frac{1}{e^{E/T}-1}, \tag{20}$$

where in the absence of a chemical potential for the fermions the Fermi-Dirac-distributions for quarks and antiquarks coincide. The effective energies are defined by

$$\begin{aligned} E_q^2&=k^2+p_F^2+M_q^2(\sigma,\vec{\pi}^2),\\ E_i^2&=k^2+p_B^2+M_i^2(\sigma,\vec{\pi}^2). \end{aligned} \tag{21}$$

The parameter a in the cutoff function is given by $a=2$ in the finite volume, in order to ensure that we can compare with the results in infinite volume. In the limit of vanishing temperature $T=0$, we find in $d=4$ the finite volume

evolution equation of the meson potential:

$$k\frac{\partial}{\partial k}U_k(\sigma,\vec{\pi}^2,L)=\frac{3}{16}\frac{k^6}{L^3}\sum_{\vec{n}}\left\{-\frac{4N_cN_f}{[E_q(\vec{n},L)]^5}+\sum_{i=1}^{4}\frac{1}{[E_i(\vec{n},L)]^5}\right\}. \tag{22}$$

The polynomial ansatz for the meson potential is determined by the following idea: Since the current quark mass is the only source of symmetry breaking, the quark term in the flow equation determines the symmetry-breaking terms of the potential. The constituent quark mass can be expanded around a finite expectation value of the mesonic fields, which is chosen in the direction of the field σ,

$$\begin{aligned}M_q^2&=g^2[(\sigma+m_c)^2+\vec{\pi}^2]\\&=g^2[(\sigma+\sigma_0-\sigma_0+m_c)^2+\vec{\pi}^2]\\&=g^2[(\sigma_0+m_c)^2+2m_c(\sigma-\sigma_0)+(\sigma^2+\vec{\pi}^2-\sigma_0^2)].\end{aligned} \tag{23}$$

We have rescaled m_c by a factor g for convenience, so that the physical current quark mass is given by gm_c. From this expression, we read off that the contributions to the potential from the fermionic terms in the flow equations can all be expressed in terms of powers of the combinations $(\sigma^2+\vec{\pi}^2-\sigma_0^2)$ for the symmetric part and $(\sigma-\sigma_0)$ for the symmetry-breaking parts. Therefore, we make for the meson potential the ansatz

$$U_k(\sigma,\vec{\pi}^2)=\sum_{i=0}^{N_\sigma}\sum_{j=0}^{[\frac{1}{2}(N_\sigma-i)]}a_{ij}(k)(\sigma-\sigma_0)^i(\sigma^2+\vec{\pi}^2-\sigma_0^2)^j. \tag{24}$$

The flow equations for the coefficients in this potential are derived in the appendix.

Incorporating the explicit breaking of the chiral symmetry into the potential and the flow from the start has several advantages. The polynomial expansion above evolves automatically from a potential with small symmetry breaking peaked around $\langle\sigma\rangle\approx 0$ to a potential with large symmetry breaking peaked at a value $\langle\sigma\rangle\approx f_\pi$. Without explicit symmetry breaking, the polynomial expansion in ϕ^2 has to be changed from a parametrization in terms of powers of ϕ^2 to $(\phi^2-\phi_0^2)$ at the chiral symmetry-breaking scale [22].

As is well known, a linear symmetry-breaking term remains unchanged in the renormalization group flow [31]. Therefore the usual strategy is to evolve the potential without a symmetry-breaking term. Explicit symmetry breaking is then taken into account after the quantum fluctuations have been integrated out on all scales [22,32,33]. In an infinite volume and for small quark masses, this is perfectly acceptable and will yield the correct results. In a finite volume, however, the situation is different. Since chiral symmetry is not spontaneously broken, explicit symmetry breaking has to be included on all scales in the renormalization group flow to obtain a nonzero value for the order parameter. Otherwise, divergences from massless Goldstone bosons would restore the symmetry. In this context, we would like to point out that even in the absence of a symmetry-breaking term, the pion decay constant does not remain zero on all renormalization scales k. On some intermediate scale below the chiral symmetry-breaking scale, $k<k_\chi$, where the quantum fluctuations are only partially integrated out, it acquires a nonzero expectation value, and chiral symmetry is spontaneously broken. However, the emergence of exactly massless Goldstone bosons dominates the infrared evolution of the potential and counteracts the formation of a symmetry-breaking condensate.

When the potential is expanded in a polynomial in a theory with exactly massless Goldstone bosons, divergences appear in the flow equations for the coefficients of operators of mass dimension higher than four [24]. As an added benefit of including explicit symmetry breaking, the presence of a finite pion mass regulates these IR divergences.

IV. NUMERICAL EVALUATION

We have solved the RG-flow equations numerically and present the results for the volume dependence of the pion mass and the pion decay constant in the following section. For the numerical evaluation, we have used the polynomial ansatz for the effective potential given in Eq. (24), and expanded up to fourth order in the fields:

$$\begin{aligned}U_k(\sigma,\vec{\pi}^2)=&\,a_{00}(k)+a_{01}(k)(\sigma^2+\vec{\pi}^2-\sigma_0^2)\\&+a_{02}(k)(\sigma^2+\vec{\pi}^2-\sigma_0^2)^2\\&+a_{10}(k)(\sigma-\sigma_0)+a_{20}(k)(\sigma-\sigma_0)^2\\&+a_{30}(k)(\sigma-\sigma_0)^3+a_{40}(k)(\sigma-\sigma_0)^4\\&+a_{11}(k)(\sigma-\sigma_0)(\sigma^2+\vec{\pi}^2-\sigma_0^2).\end{aligned} \tag{25}$$

Here, we first discuss our choice of model parameters at the UV scale, and some details of the numerical evaluation.

The UV scale itself is determined from physical considerations as the scale below which a description of QCD with hadronic degrees of freedom is appropriate. Here, we choose $\Lambda_{UV}=1.5$ GeV. At the ultraviolet scale Λ_{UV}, the free parameters of the quark-meson model are the meson mass m_{UV}, the four-meson-coupling λ_{UV}, and the current quark mass gm_c, which controls the degree of explicit symmetry breaking. The Yukawa coupling g does not evolve in the present approximation [22,32,33]. We choose $g=3.26$, which leads to a reasonable constituent quark mass of $M_q=g(f_\pi+m_c)\approx 310$ MeV for physical values for the pion decay constant $f_\pi=93$ MeV and the current quark mass $gm_c=7$ MeV.

In Table I, we summarize the three parameter sets which we used in obtaining our results for pion masses of 100, 200, and 300 MeV. We determine these UV parameters by fitting to a particular value for the pion mass $m_\pi(\infty)$ and to the corresponding value for the pion decay constant $f_\pi(\infty)$ in infinite volume. We then evolve the RG equations with these parameters to predict the volume dependence of $f_\pi(L)$ and $m_\pi(L)$.

For any value of the pion mass, the corresponding value of the pion decay constant is taken from chiral perturbation theory [9]. The pion mass is mainly controlled by the value of the current quark mass, which parametrizes the symmetry breaking. The current quark mass varies from approximately 2 MeV for a pion mass of 100 MeV to about 10 MeV for $m_\pi = 200$ MeV, it has to be increased to approximately 25 MeV for $m_\pi = 300$ MeV. To achieve the correct corresponding values for the pion decay constant, the meson mass at the UV scale has to be decreased from approximately $m_{UV} = 780$ MeV to $m_{UV} = 700$ MeV, while the pion mass increases from 100 to 300 MeV. The four-meson-coupling λ_{UV} is fixed. We have checked that our results are to a very large degree independent of the particular choice of UV parameters: Different sets of parameters leading to the same values of the low-energy constants in the infinite volume give the same volume dependence.

Although it facilitates the comparison to chiral perturbation theory, it is not necessary as a matter of principle to use the chiral perturbation theory result for the mass dependence of the pion decay constant. However, as has been found for infinite volume, in order to correctly describe the behavior of the pion decay constant as a function of a single symmetry-breaking parameter, it is necessary to go beyond the approximation of a constant expectation value for the meson field, which we used in this paper, and to include wave function renormalizations in the RG flow [27]. This makes it possible to recover the correct prefactors of chiral logarithms in the framework of the renormalization group. Such an approach is more powerful than the present one, since in addition to the volume dependence, it predicts the dependence of m_π and f_π on the symmetry-breaking parameter m_c. We stress that even in such an approach, it remains necessary to fit the parameters at the UV scale to the correct values of the low-energy constants. Thus, for example, the value of the pion decay constant in the chiral limit is not a prediction of the model, but a necessary input to constrain its parameters. The full set of RG equations including the wave function renormalization and coupling constant renormalization equations would reduce the input parameters to the four-fermion coupling and the current quark mass at the UV scale. In connection with the symmetry-breaking ansatz Eq. (24), these equations are more complicated and have not been worked out yet.

TABLE I. Values for the parameters at the UV scale used in the numerical evaluation. The parameters are determined in infinite volume by fitting to a particular pion mass and the corresponding value of the pion decay constant, taken from chiral perturbation theory. Note that in our notation, the physical current quark mass corresponds to gm_c.

Λ_{UV} [MeV]	m_{UV}[MeV]	λ_{UV}	gm_c [MeV]	f_π [MeV]	m_π [MeV]
1500	779.0	60	2.10	90.38	100.8
1500	747.7	60	9.85	96.91	200.1
1500	698.0	60	25.70	105.30	300.2

A limit on the possible values of the current quark mass is given by the requirement that all masses, in particular, the sigma-mass, remain substantially smaller than the ultraviolet cutoff $\Lambda_{UV} \approx 1500$ MeV of the model. For a pion mass of $m_\pi = 300$ MeV, we find $m_\sigma \approx 800$ MeV.

With regard to the UV-cutoff, we find only a slight dependence of our results for reasonably large volumes. When we change the cutoff from $\Lambda_{UV} = 1500$ MeV to $\Lambda_{UV} = 1100$ MeV, our results for the relative shift $R[m_\pi(L)]$ of the pion mass in the finite volume change little. The change in the pion mass from a variation of the cutoff is of the order of less than 1% for $L > 2$ fm, and approximately 6% at $L = 1$ fm for the largest pion mass we considered here, $m_\pi = 300$ MeV. For smaller pion mass, the dependence on the UV cutoff becomes weaker, for $m_\pi = 100$ MeV it is negligible on the scale of our results. This can be understood, since a higher degree of explicit symmetry breaking leads to more massive particles for which a smaller value for the UV momentum cutoff becomes more relevant.

The sums over the momentum modes in the flow equations cannot be performed analytically. For a numerical evaluation of the flow equations, these sums must be truncated at a maximal mode number $N_{\max} = \max|\vec{n}|$ which defines the cutoff momentum mode $p_{\max} = \frac{2\pi}{L} N_{\max}$. This numerical truncation should not introduce an additional UV cutoff in the model, and therefore we require that

$$\frac{2\pi}{L} N_{\max} \gg \Lambda_{UV}. \tag{26}$$

Since we use a ''soft'' cutoff function it is necessary to really satisfy the above equation with a safe margin. For the volumes with $L \geq 1$ fm considered here, we have used $N_{\max} = 40$.

In Fig. 1, the dependence of the relative difference of the pion mass in finite volume from its value in the infinite volume limit, $R[m_\pi(L)]$, is shown as a function of L for different values of the maximal mode number $N_{\max}$. The relative mass difference depends mainly on $m_\pi L$ and drops exponentially for large values of this dimensionless variable. Thus, for any given value of L, the value of $R[m_\pi(L)]$ will be smaller for a heavier pion. Comparing the two panels in Fig. 1, we see that although the absolute values

are smaller, the relative error due to the finite number of momentum modes in the evaluation is larger for a heavier pion. The reason is the increasing importance of the nonzero-momentum modes when the pion mass becomes larger at fixed box size. Following the argument from [11] outlined above, if $1/m_\pi \gg L$, then the partition function is dominated by the zero modes and effects from finite momentum modes present small corrections. When the pion mass is increased, the importance of the finite momentum modes grows and the number of modes has to be increased to obtain results with the same level of accuracy. This argument can be presented in a more formal way. The momentum sums contributing to the flow equations are of the form

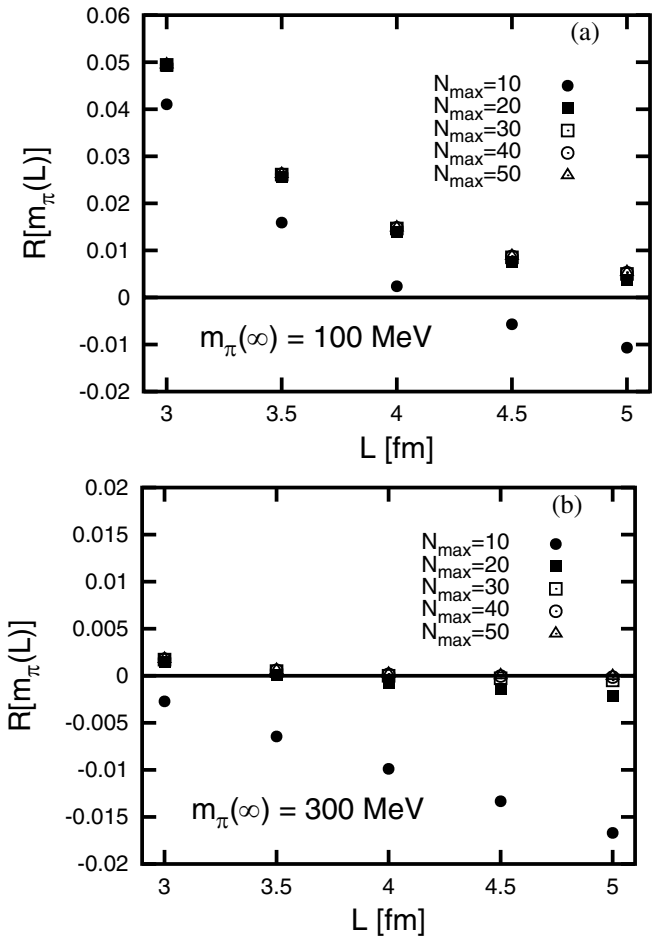

FIG. 1. The figures show the dependence of the results for the pion mass in finite volume on the truncation $N_{\max}$ of the momentum sum in the numerical evaluation of the flow equations. Plotted is $R[m_\pi(L)]$, the relative deviation of the finite volume pion mass from the value in infinite volume, as a function of the box size L, for different values of $N_{\max}$. Results for two different values of the pion mass are shown in the two panels. Ideally, for large volumes, the relative deviation from the infinite volume pion mass should approach zero. The truncation has a relatively larger effect for heavier pion masses.

$$\sum_{n_1,n_2,n_3} \frac{1}{k^2 + m_\pi^2 + \vec{n}^2 \frac{4\pi^2}{L^2}}, \tag{27}$$

where $\vec{n}^2 = n_1^2 + n_2^2 + n_3^2$. For small values of the renormalization scale k, the sum is dominated by the zero mode term

$$\frac{1}{m_\pi^2} + \frac{1}{m_\pi^2 + \frac{4\pi^2}{L^2}} + \ldots. \tag{28}$$

If the box is sufficiently small, all terms with nonzero momentum are suppressed by $1/L^2$, which acts as a large regulator. As we increase the size of the box, so that $1/L \sim m_\pi$, the contributions of the nonzero-momentum modes are of the same size as the zero mode term. Therefore, effects from a truncation of the momentum sums should be expected to appear already at a smaller box size for large pion masses, which is exactly what we observe.

V. RESULTS

The results of the RG-flow equations for the evolution with the infrared cutoff scale k give a picture of chiral symmetry breaking which reflects the formation of the quark condensate for higher momenta and the effects of pion fluctuations at low scales. Figure 2 shows the masses of the pion and sigma, and the pion decay constant as a function of the renormalization scale k, for a value of $m_\pi = 100$ MeV, in the infinite volume limit. Starting at the UV scale Λ_{UV} and proceeding towards smaller values of k, we observe that the pion decay constant f_π grows rapidly around the chiral symmetry-breaking scale $k_{\chi SB} \sim$ 800 MeV, begins to flatten between 600–400 MeV, and becomes almost completely flat below 300 MeV. Generally, massive degrees of freedom decouple from the renormalization group flow at a momentum scale given by the value of their mass m, i.e., they do not contribute to the renormalization for $k < m$. This can be seen clearly in the flow of f_π. As soon as the renormalization scale is of the order of the constituent quark mass (approximately 300 MeV), the quarks are no longer dynamical degrees of freedom and f_π becomes essentially constant. The RG-flow of the mass of the heaviest meson, the sigma, is in several respects very similar to the flow of f_π. Its slope is also initially large at the chiral symmetry-breaking scale and starts to decrease between 600–400 MeV as well. The value of the sigma-mass reaches a maximum at k slightly above 300 MeV. Its decrease below this scale is due to the light pion with a mass of 100 MeV, which remains in the evolution as the only dynamical degree of freedom. When the pion mass is increased, the drop in the sigma-mass below the scale set by the constituent quark mass becomes much less pronounced. For $m_\pi \approx m_q \approx 300$ MeV, $m_\sigma(k)$ is essentially a flat function of k after it has reached its maximum.

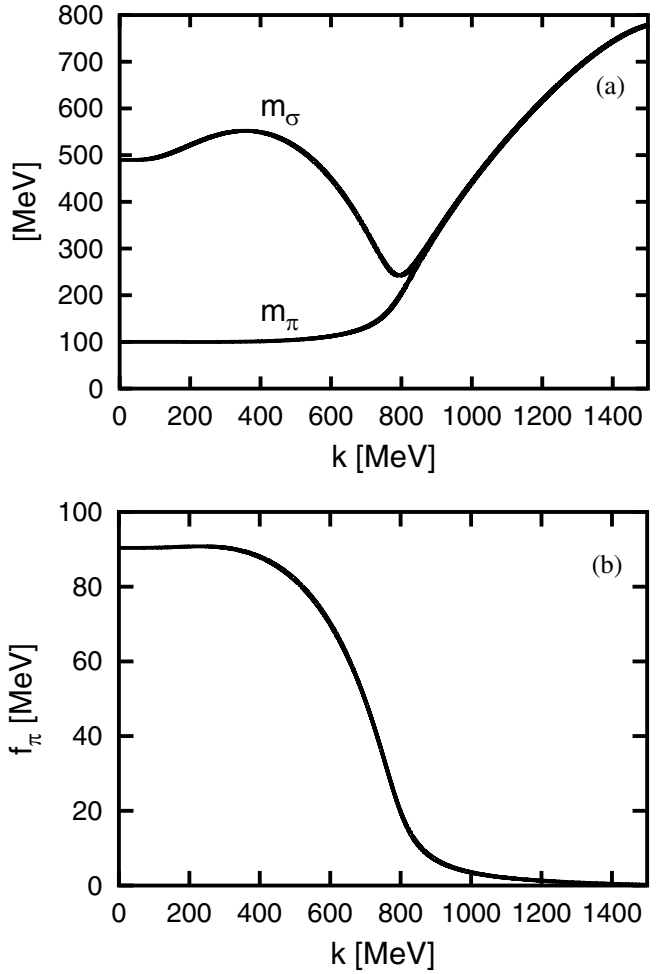

FIG. 2. Masses of the mesonic degrees of freedom and the pion decay constant as a function of the renormalization scale k in infinite volume. The chiral symmetry-breaking scale can be clearly identified as the scale at which the mass of the heaviest meson (the σ) has a minimum. For this figure, we have chosen $m_\pi(\infty) = 100$ MeV and $f_\pi(\infty) = 90.4$ MeV.

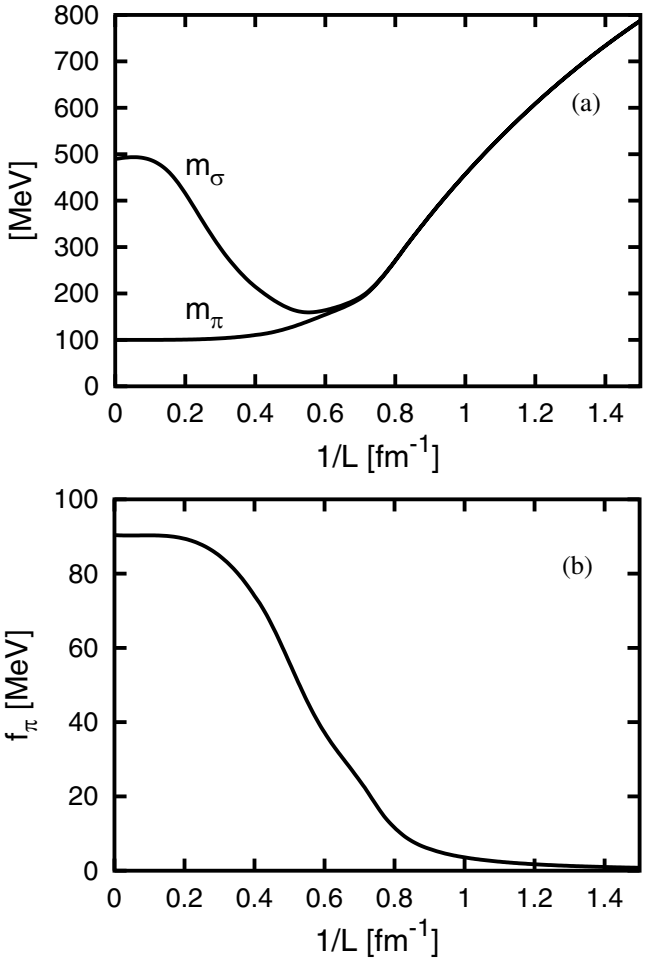

FIG. 3. Masses of the mesonic degrees of freedom and the pion decay constant as a function of the inverse box size $1/L$. The results are obtained by completely integrating out all quantum fluctuations ($k \to 0$) at fixed L. As soon as $k < 1/L$, the box size becomes the controlling scale, and in the limit $k \to 0$ it is the only scale that remains. As for the preceding figures, we show the results with $m_\pi = 100$ MeV and $f_\pi = 90.4$ MeV for $k \to 0$ and $L \to \infty$.

In finite volume, a similar behavior is visible. In Fig. 3, the meson masses and the pion decay constant are shown as a function of the scale $1/L$ set by the finite volume. In these results, all quantum fluctuations are integrated out completely, which removes the scale k. Now let us consider a finite value of k, where the quantum fluctuations are only partially integrated out. The scale $1/L$ introduced by the finite volume is in competition with the renormalization scale k. As soon as k drops below π/L, the renormalization scale no longer controls the renormalization flow. We can interpret the results shown in Fig. 3 roughly as an instant picture of the k-flow arrested at a scale $k = \pi/L$. However, this correspondence is not one-to-one: while the cutoff k affects both bosonic and fermionic fields in the same way, this is not true for $1/L$. Since there are no zero modes for fields with antiperiodic boundary conditions, the fermionic fields are more strongly affected by this cutoff than the mesons. For the mesons, the scale $\frac{2\pi}{L}$ imposes only a minimum value for the smallest nonzero-momentum mode. For the fermionic fields, on the other hand, the lowest momentum mode $\sqrt{3}\pi/L$ can effectively ''freeze'' the quark fields already above the constituent quark mass scale and no condensation of quarks takes place. For very small volumes $1/L > 0.5$ fm^{-1}, the suppression of quark condensation by the large cutoff becomes the dominating effect. The chiral symmetry is approximately restored. A more subtle effect can also be seen in the behavior of the sigma-mass. While the sigma-mass has a maximum in the k-flow at a value of $m_\sigma \approx 600$ MeV, from which it drops to $m_\sigma \approx 500$ MeV due to the pion fluctuations, there is no corresponding maximum in the $1/L$-dependence. With decreasing $1/L$ the pions hardly feel the constraints of the finite volume, but the momentum

scale at which the quarks decouple consistently increases. Therefore the pion contributions at low momenta have a greater effect in the RG-flow, since the k-region increases in which they are the only relevant degrees of freedom. Through this effect, the pions also contribute toward the restoration of chiral symmetry for small volumes.

The volume dependence of the low-energy observables is the main result of this paper. In Table II, we give the values for $R[m_\pi(L)]$ cf. eq. (1), the relative difference of the pion mass $m_\pi(L)$ in finite volume from $m_\pi(\infty)$, its value in infinite volume, for three volume sizes $L = 2.0$, 2.5, 3.0 fm and three pion masses $m_\pi(\infty) = 100$, 200, 300 MeV.

In Figs. 4 and 5, we show the relative change of the pion mass $m_\pi(L)$ and the pion decay constant $f_\pi(L)$ as a function of the size L of the three-dimensional volume. We plot the results for the relative differences on a logarithmic scale for three different values of the pion mass $m_\pi(\infty) =$ 100, 200, 300 MeV.

Let us first discuss the plots for the pion mass in Fig. 4. The relative change of the pion mass decreases with the volume size L and the pion mass $m_\pi(\infty)$. Figure 4 also contains the results of chiral perturbation theory from the exact one-loop calculation in finite volume [10] and also the ''best estimate'' from [9]. As discussed in section II, the difference between the results of Lüscher's formula for the mass shift which uses as input $\pi\pi$-scattering in the one-(*lo*) and three-(*nnlo*) loop order is used as a correction to the *exact* one-loop mass shift from [10].

Our RG results have the same slope as those from chiral perturbation theory, but are consistently above chiral perturbation theory, even with corrections to three loops. In general, the RG calculation gives values for $R[m_\pi(L)]$ which are about a factor 1.5 to 2.0 larger than the values from chPT, as can be seen in Table II.

The difference between the RG result and the loop expansion decreases with higher order in loops. The RG result is closer to the calculation with *nnlo*-Lüscher formula than to the one-loop chPT calculation.

For large volumes, the pion mass should drop as $\exp(-m_\pi L)$. Therefore, we expect that the slope of the RG result is the same as that from chiral perturbation theory, which is indeed the case. The calculation with the flow equation can be continued to smaller box sizes, as long as the momenta constrained by the box are below the cutoff Λ_{UV}. The slope of the RG result at small box size ($L < 1$ fm) is approximately given by the meson mass $m_\sigma = m_\pi$ cf. Fig. 3, after the transition between the regime dominated by chiral symmetry breaking and the one with restored chiral symmetry has taken place. In this other region the chiral expansion can no longer be considered reliable and is therefore no longer applied.

While the relative difference between the exact one-loop result and the RG results remains approximately constant for different pion masses, the relative difference between the RG results and the results of Colangelo and Dürr [9] decreases when the mass of the pion is increased. We have checked that the difference between our RG results and the chiral perturbation theory results from Colangelo and Dürr are consistent with the error estimate of Lüscher's approximation formula. We find for all pion masses that the differences decrease exponentially according to $\exp(-Cm_\pi L)$, with C a positive constant of order 1.

Next we discuss the results for the volume dependence of the pion decay constant shown in Fig. 5. As for the pion mass, we compare with the chiral perturbation theory results [8,10]. Note that in this case, we define the relative difference with opposite sign as $R[f_\pi(L)] = [f_\pi(\infty) - f_\pi(L)]/f_\pi(\infty)$, because the pion decay constant is *smaller* for a finite volume, in contrast to the pion mass. We refer to Fig. 3 for an illustration of the global behavior of $f_\pi(L)$. When the size of the volume is decreased, the pion decay constant at first drops only slowly, and then sharply at the scale associated with chiral symmetry breaking. For very

TABLE II. Values for $R[m_\pi(L)]$ cf. eq. (1), the relative shift of the pion mass in finite volumes of $L = 2.0$, 2.5, 3.0 fm, compared to the value in infinite volume, for pion masses of $m_\pi(\infty) = 100$, 200, 300 MeV. We compare our RG calculation to the exact one-loop chPT results of [11] for a finite volume (1L chPT), and the exact one-loop calculation with corrections in three-loop order obtained with chPT using Lüscher's formula [9] [1L chPT + (*nnlo-lo*)]. In the last column, the difference ΔR between the RG result and the three-loop corrected chPT result is given.

			$R[m_\pi(L)]$			
L [fm]	$m_\pi(\infty)$ [MeV]	$m_\pi L$	RG	1L chPT	+(*nnlo-lo*)	ΔR
2.0	100	1.01293	26.6×10^{-2}	8.74×10^{-2}	11.6×10^{-2}	15.0×10^{-2}
	200	2.02586	5.38×10^{-2}	2.00×10^{-2}	3.31×10^{-2}	2.07×10^{-2}
	300	3.03879	1.70×10^{-2}	0.56×10^{-2}	1.12×10^{-2}	0.58×10^{-2}
2.5	100	1.26616	10.37×10^{-2}	3.85×10^{-2}	4.97×10^{-2}	5.40×10^{-2}
	200	2.53233	1.95×10^{-2}	0.73×10^{-2}	1.17×10^{-2}	0.78×10^{-2}
	300	3.79849	5.31×10^{-3}	1.65×10^{-3}	3.27×10^{-3}	2.04×10^{-3}
3.0	100	1.5194	4.94×10^{-2}	1.91×10^{-2}	2.41×10^{-2}	2.53×10^{-3}
	200	3.03879	7.85×10^{-3}	2.95×10^{-3}	4.65×10^{-3}	3.20×10^{-3}
	300	4.55819	1.76×10^{-3}	0.54×10^{-3}	1.05×10^{-3}	0.71×10^{-3}

small volumes, the pion decay constant vanishes and chiral symmetry is effectively restored. This is true for $L \to 0$ regardless of the value of the pion mass. Therefore, the largest possible relative shift for $L \to 0$ is $R[f_\pi(0)] = 1$, when the order parameter vanishes completely.

The plots for the volume dependence of f_π illustrate in which region chiral perturbation theory remains valid. Since spontaneously broken chiral symmetry and a sufficiently large f_π are required, chPT does not describe the transition to the region with effectively restored chiral

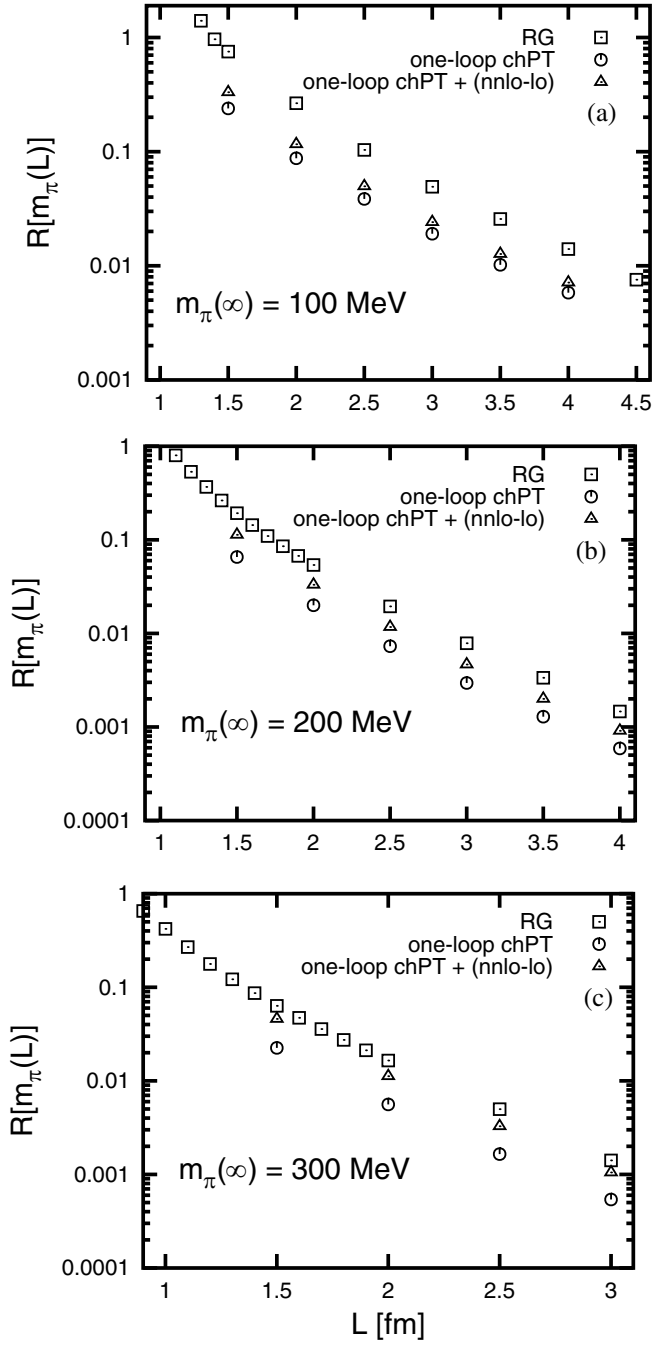

FIG. 4. Volume dependence of the pion mass. We plot the relative shift of the pion mass from its infinite volume limit $R[m_\pi(L)] = [m_\pi(L) - m_\pi(\infty)]/m_\pi(\infty)$ as a function of the size of the volume L. For comparison, we also plot the results from chPT calculations taken from [9]. The values for the pion mass in infinite volume are given in the figure, note the different scales on the axes for different $m_\pi(\infty)$.

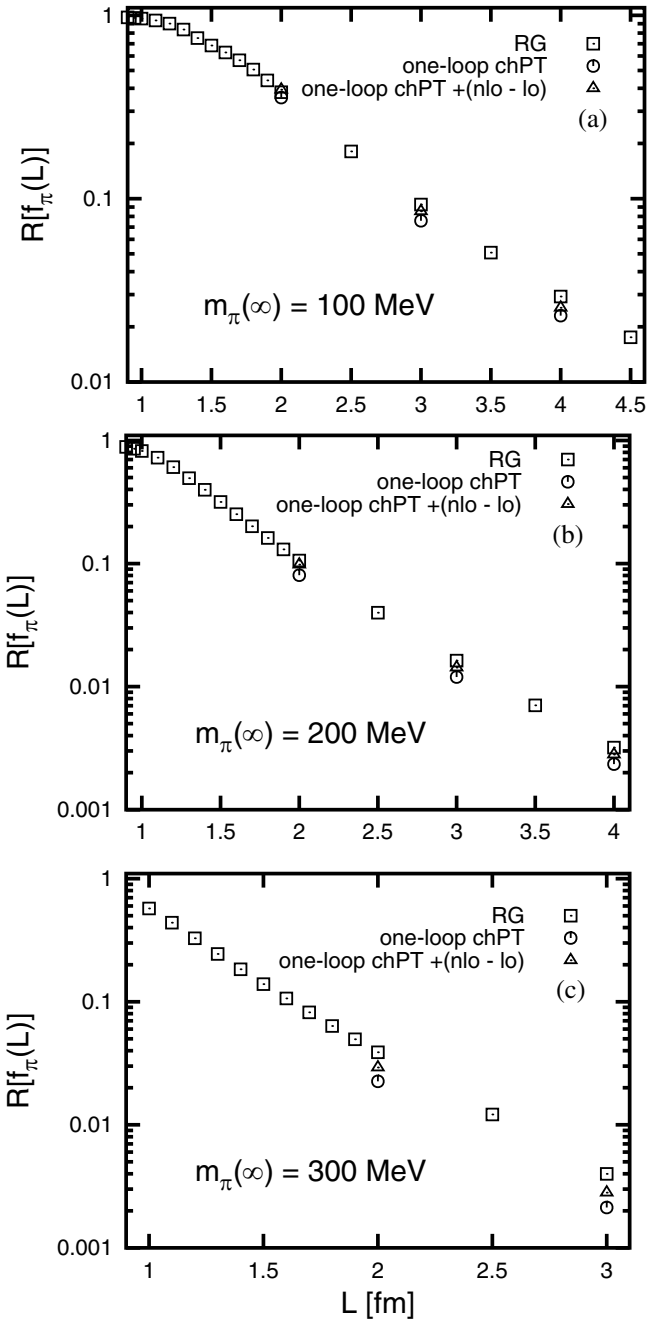

FIG. 5. Volume dependence of the pion decay constant. We plot the relative shift from the infinite volume limit $R_{f_\pi}(L) = [f_\pi(\infty) - f_\pi(L)]/f_\pi(\infty)$ as a function of the box size L for different values of the pion mass. For comparison, we show the chPT results taken from [8]. The values for $m_\pi(\infty)$ are given in the panels. Note the different scales on the axes for different $m_\pi(\infty)$.

symmetry. Therefore, chiral perturbation theory results are available only for volumes with $L \geq 2$ fm. Already for $L = 2$ fm and a pion mass $m_\pi = 100$ MeV, the f_π-shift is almost 40%. The RG method remains valid in both regions, down to very small volumes.

We compare with the chiral perturbation theory results obtained by using an approximation similar to Lüscher's formula for the pion mass shift, which was derived in [8]. For the pion decay constant, the input needed to calculate the finite volume shift is an amplitude involving the axial current in infinite volume. So far only two loops in chiral perturbation theory (*nlo*) are known. The chPT *nlo*-corrections to the exact one-loop result increase the shift towards larger values. As in the case of the pion mass, the RG results give a slightly larger finite volume shift than the chPT results. Again the results from RG and chPT converge for larger values of the pion mass (note the different scales on both axes in the plots for different values of m_π!).

For the volume dependence of the sigma-mass, we refer back to Fig. 3, where we show the overall dependence of m_σ on $1/L$. It is interesting to relate the variation of $m_\sigma(1/L)$ to the 0^{++} phase shift of $\pi\pi$-scattering, which will be done in a separate work.

VI. CONCLUSIONS

We have presented a new approach to the quark-meson model employing the renormalization group method in a finite volume within the framework of the Schwinger proper time formalism. Central to any such approach is the inclusion of explicit chiral symmetry breaking. Since chiral symmetry is not broken spontaneously in a finite volume, it is necessary to introduce a finite current quark mass. In this paper, we have evolved the effective potential with additional symmetry-breaking terms. The form of these terms is constrained by the quark contributions to the renormalization group flow, which introduce the explicit chiral symmetry breaking.

By solving the resulting renormalization group flow equations numerically, we have obtained results for the volume dependence of the meson masses, in particular the pion mass, and the pion decay constant, the order parameter of chiral symmetry breaking.

Our results show consistently a larger finite volume mass shift for the pion than has been obtained in chiral perturbation theory including up to three loops. The differences between the chiral perturbation theory results which make use of the Lüscher formula and the RG results obtained in the present paper are consistent with the error estimate for Lüscher's approximation. As one expects, the difference is largest for small values of $m_\pi L$. We have checked that this difference decreases exponentially with an increase in this dimensionless quantity. As shown in figs. 4 and 5, our results and those obtained in chiral perturbation theory with Lüscher's formula [8,9] converge for large current quark masses. We note that the ratio of the results from chPT and RG does not depend on L, even down to $L = 1.5$ fm.

Compared to the present numerical approach, chiral perturbation theory has the advantage that it is possible to obtain analytical expressions for the finite volume mass shift. This makes comparisons to lattice results simpler. On the other hand, current lattice volumes and lattice pion masses are at the edge of a reliable chiral perturbation theory calculation. In contrast, the RG method remains valid for large current quark masses as well as small volumes.

The main uncertainty of the RG method comes from its dependence on the UV cutoff scale Λ_{UV} for large meson masses. The system becomes sensitive to Λ_{UV} for large explicit symmetry breaking, because the mass of the sigma as the heaviest particle approaches the UV cutoff. For a pion mass of $m_\pi = 300$ MeV, the sigma-mass is $m_\sigma \approx 800$ MeV. In this case, a cutoff variation between $\Lambda_{UV} = 1500$ MeV and 1100 MeV, changes the pion mass for a volume with $L = 1$ fm by approximately 6%, and by less than 1% for $L > 2$ fm. Within this uncertainty, our results agree with those of chPT for $m_\pi = 300$ MeV. In contrast, for $m_\pi = 100$ MeV the cutoff dependence is so weak that it is not noticeable on the scale of the results. The RG and chPT results do not agree within this uncertainty, cf. Table II for $m_\pi = 100$ MeV and $m_\pi = 200$ MeV.

The dependence of our results on the choice of model parameters at the UV scale is much weaker than that on the cutoff. By fitting to the values of the low-energy observables m_π and f_π in infinite volume, we achieve a very high degree of independence on the particular choice of UV parameters.

We expect that the inclusion of wave function renormalizations in the finite volume renormalization group flow should make it possible to describe the low-energy constants as a function of a single symmetry-breaking parameter, the quark mass m_c. It has already been observed that this is the case in infinite volume, where the behavior of m_π and f_π as a function of m_c is described correctly when all other UV parameters remain fixed [27]. Systematic errors introduced by the simplification used in this paper to adjust both $m_\pi(\infty)$ and $f_\pi(\infty)$ in infinite volume could then be estimated by a comparison of the calculations.

Although we have not yet investigated these questions in depth, it appears that the present approach, which treats the pion fields and the sigma explicitly and as individual degrees of freedom, improves the convergence [24] of the polynomial expansion of the effective potential. This is due to the finite mass acquired by the Goldstone bosons, which becomes relevant for $k \to 0$.

The RG approach shows in a transparent way the relevance of the momentum scale introduced by the finite volume for the quantum fluctuations.

ACKNOWLEDGMENTS

H. J. P. would like to thank Professor Leutwyler and Dr. Dürr for instructive discussions. J. B. would like to thank the GSI for financial support.

APPENDIX A: FLOW EQUATIONS

We derive flow equations for the coefficients of the potential by inserting Eq. (24) into the flow equation for the potential and comparing coefficients of both sides. We define expansion coefficients for the flow equations:

$$\left(k\frac{\partial}{\partial k}U_k\right)^{ij} := \frac{1}{i!}\frac{1}{j!}\left(\frac{\partial}{\partial\sigma}\right)^i\left(\frac{\partial}{\partial\vec{\pi}^2}\right)^j k\frac{\partial}{\partial k}U_k\Big|_{\substack{\sigma=\sigma_0\\ \vec{\pi}^2=0}}. \quad \text{(A1)}$$

Then the flow equations for the coefficients a_{ij} in the ansatz for the potential are given by

$$\begin{aligned}\left(k\frac{\partial}{\partial k}U_k\right)^{ij} &= \left(k\frac{\partial}{\partial k}a_{ij}\right) + a_{i+1,j}\left(-k\frac{\partial\sigma_0}{\partial k}\right)(i+1)\\ &\quad\times(1-\delta_{N_\sigma,i}) + a_{i,j+1}(j+1)\left(-2\sigma_0 k\frac{\partial\sigma_0}{\partial k}\right)\\ &\quad\times(1-\delta_{\frac{1}{2}(N_\sigma-i),j}) \quad \text{(A2)}\end{aligned}$$

with the additional condition that $(1+2j)\le N_\sigma$.

In order for $\sigma=\sigma_0$ to actually correspond to a minimum of the potential, it must satisfy $\frac{\partial}{\partial\sigma}U_k|_{\sigma=\sigma_0}=0$. For the coefficients a_{10} and a_{01}, this translates into the condition

$$a_{10} + 2a_{01}\sigma_0 \equiv 0. \quad \text{(A3)}$$

Because of this condition, only two of the variables in the set $\{a_{10}, a_{01}, \sigma_0\}$ are independent, and the third one can be expressed in terms of the other two. Likewise, if we take the derivative of the Eq. (A3) with respect to the renormalization scale k, we get an equation which relates the flow of these three variables:

$$k\frac{\partial}{\partial k}a_{10} + 2a_{01}k\left(\frac{\partial}{\partial k}\sigma_0\right) + 2\sigma_0 k\frac{\partial}{\partial k}a_{01} = 0. \quad \text{(A4)}$$

We can use this equation to replace the flow equation for a_{10} in the above set Eq. (A2). It is desirable to eliminate a_{10}, since σ_0 and a_{01} both correspond to the observables we wish to obtain, namely, the pion decay constant and the pion mass. In addition, with this replacement the system of differential equations can also be solved more easily.

From the general expression for the flow equations Eq. (A2), we find the particular equations governing a_{10} and a_{01}:

$$\begin{aligned}\left(k\frac{\partial}{\partial k}U_k\right)^{10} &= k\frac{\partial}{\partial k}a_{10} - 2a_{20}\left(k\frac{\partial}{\partial k}\sigma_0\right)\\ &\quad - a_{11}\left(2\sigma_0 k\frac{\partial}{\partial k}\sigma_0\right), \quad \text{(A5)}\end{aligned}$$

$$\begin{aligned}\left(k\frac{\partial}{\partial k}U_k\right)^{01} &= k\frac{\partial}{\partial k}a_{01} - a_{11}\left(k\frac{\partial}{\partial k}\sigma_0\right)\\ &\quad - 2a_{02}\left(2\sigma_0 k\frac{\partial}{\partial k}\sigma_0\right). \quad \text{(A6)}\end{aligned}$$

The flow equation for a_{10} contains on the left-hand side (LHS) only terms that are proportional to the symmetry-breaking current quark mass m_c. Because of this, a_{10} does not evolve in the chiral limit $m_c\to 0$. If it is initially zero at the UV scale, it remains zero on all scales. In this case, the condition (A4) forces the coefficient a_{01} to vanish as soon as σ_0 acquires a finite expectation value. This corresponds to the appearance of exactly massless Goldstone bosons in case of spontaneous symmetry breaking, in accordance with our expectations for the chiral limit.

In order to derive a flow equation for the minimum of the potential σ_0, we can combine the two equations and use Eq. (A4) to eliminate the k-derivatives of a_{10} and a_{01}:

$$\begin{aligned}&\left(k\frac{\partial}{\partial k}U_k\right)^{10} + 2\sigma_0\left(k\frac{\partial}{\partial k}U_k\right)^{01}\\ &\quad = -\left(k\frac{\partial}{\partial k}\sigma_0\right)(2a_{20} + 2a_{01} + 4a_{11}\sigma_0 + 8a_{02}\sigma_0^2).\end{aligned} \quad \text{(A7)}$$

From the expressions for the meson masses, evaluated at the minimum of the potential, it can be seen that the expression in brackets, which multiplies the k-derivative of σ_0, is up to a constant factor the square of the σ-mass, M_σ^2. Therefore, this equation is always well-conditioned. The only exception is at the chiral symmetry-breaking scale, where M_σ^2 drops sharply, if the explicit symmetry breaking is very small. For reasonably large pion masses, this is not a problem.

APPENDIX B: ANSATZ FOR THE POTENTIAL

We use the flow equations in infinite volume to motivate the ansatz for the potential with explicit symmetry breaking. Neglecting the mesonic contributions to the flow equations, we are left with the terms arising from the fermions:

$$k\frac{\partial}{\partial k}U^F(\sigma,\vec{\pi}^2) = -\frac{4N_f N_c}{32\pi^2}\frac{k^6}{k^2+M_q^2}. \quad \text{(B1)}$$

The constituent quark mass M_q contains through the current quark mass m_c the only explicitly symmetry-breaking term in the flow equation. As shown in Eq. (23), by expanding around the minimum of the potential, the quark mass can be written as

$$M_q^2 = g^2[(\sigma_0 + m_c)^2 + 2m_c(\sigma - \sigma_0) + (\sigma^2 + \vec{\pi}^2 - \sigma_0^2)], \tag{B2}$$

where m_c is rescaled by a factor of g for convenience. When we expand the denominator in the flow equation in the deviation of the fields from the vacuum expectation value, the result contains only those terms we postulated in our ansatz for the potential:

$$\begin{aligned} k\frac{\partial}{\partial k}U^F(\sigma, \vec{\pi}^2) = &-\frac{1}{32\pi^2}4N_fN_c\frac{k^6}{k^2 + g^2(\sigma_0 + m_c)^2} \times \left\{(\sigma^2 + \vec{\pi}^2 - \sigma_0^2)\left[-\frac{g^2}{k^2 + g^2(\sigma_0 + m_c)^2}\right] + (\sigma^2 + \vec{\pi}^2 - \sigma_0^2)^2\right. \\ &\times \left[\left(\frac{g^2}{k^2 + g^2(\sigma_0 + m_c)^2}\right)^2\right] + (\sigma - \sigma_0)\left[-2m_c\left(\frac{g^2}{k^2 + g^2(\sigma_0 + m_c)^2}\right)\right] + (\sigma - \sigma_0)^2 \\ &\left.\times \left[4m_c^2\left(\frac{g^2}{k^2 + g^2(\sigma_0 + m_c)^2}\right)^2\right] + (\sigma - \sigma_0)(\sigma^2 + \vec{\pi}^2 - \sigma_0^2)2\left[-2m_c\left(\frac{g^2}{k^2 + g^2(\sigma_0 + m_c)^2}\right)^2\right] + \ldots\right\}. \end{aligned} \tag{B3}$$

All remaining terms are of higher order in $(\sigma - \sigma_0)$ or $(\sigma^2 + \vec{\pi}^2 - \sigma_0^2)$ or any combination thereof. Only the terms in $(\sigma^2 + \vec{\pi}^2 - \sigma_0^2) = (\phi^2 - \sigma_0^2)$ remain in the chiral limit $m_c \to 0$. These terms respect the chiral symmetry and the potential reduces to the symmetric form.

[1] D. Becirevic and G. Villadoro, Phys. Rev. D **69**, 054010 (2004).
[2] QCDSF-UKQCD Collaboration, A. Ali Khan *et al.*, Nucl. Phys. B **689**, 175 (2004).
[3] Zeuthen-Rome (ZeRo) Collaboration, M. Guagnelli, K. Jansen, F. Palombi, R. Petronzio, A. Shindler, and I. Wetzorke, Phys. Lett. B **597**, 175 (2004).
[4] D. Arndt and C. J. D. Lin, Phys. Rev. D **70**, 014503 (2004).
[5] M. Procura, T. R. Hemmert, and W. Weise, Phys. Rev. D **69**, 034505 (2004).
[6] S. R. Beane and M. J. Savage, Phys. Rev. D **70**, 074029 (2004).
[7] M. E. Berbenni-Bitsch, A. D. Jackson, S. Meyer, A. Schäfer, J. J. M. Verbaarschot, and T. Wettig, Nucl. Phys. (Proc. Suppl.) **63**, 820 (1998).
[8] G. Colangelo and C. Haefeli, Phys. Lett. B **590**, 258 (2004).
[9] G. Colangelo and S. Dürr, Eur. Phys. J. C **33**, 543 (2004).
[10] J. Gasser and H. Leutwyler, Phys. Lett. B **184**, 83 (1987).
[11] J. Gasser and H. Leutwyler, Phys. Lett. B **188**, 477 (1987).
[12] J. Gasser and H. Leutwyler, Nucl. Phys. B **307**, 763 (1988).
[13] H. Leutwyler and A. Smilga, Phys. Rev. D **46**, 5607 (1992).
[14] J. Gasser and H. Leutwyler, Ann. Phys. (N.Y.) **158**, 142 (1984).
[15] E. V. Shuryak and J. J. M. Verbaarschot, Nucl. Phys. A **560**, 306 (1993).
[16] J. J. M. Verbaarschot, Phys. Rev. Lett. **72**, 2531 (1994).
[17] J. J. M. Verbaarschot, Phys. Lett. B **368**, 137 (1996).
[18] P. H. Damgaard, R. G. Edwards, U. M. Heller, and R. Narayanan, Nucl. Phys. (Proc. Suppl.) **83**, 434 (2000).
[19] P. H. Damgaard, R. G. Edwards, U. M. Heller, and R. Narayanan, Phys. Rev. D **61**, 094503 (2000).
[20] M. E. Berbenni-Bitsch, S. Meyer, A. Schäfer, J. J. M. Verbaarschot, and T. Wettig, Phys. Rev. Lett. **80**, 1146 (1998).
[21] P. H. Damgaard, U. M. Heller, and A. Krasnitz, Phys. Lett. B **445**, 366 (1999).
[22] B. J. Schaefer and H. J. Pirner, Nucl. Phys. A **660**, 439 (1999).
[23] J. Meyer, K. Schwenzer, H. J. Pirner, and A. Deandrea, Phys. Lett. B **526**, 79 (2002).
[24] G. Papp, B. J. Schaefer, H. J. Pirner, and J. Wambach, Phys. Rev. D **61**, 096002 (2000).
[25] B. J. Schaefer and J. Wambach, nucl-th/0403039.
[26] D. U. Jungnickel and C. Wetterich, Eur. Phys. J. C **2**, 557 (1998).
[27] L. Jendges, K. Schwenzer, and H. J. Pirner (in preparation).
[28] M. Lüscher, Commun. Math. Phys. **104**, 177 (1986).
[29] J. Meyer, G. Papp, H. J. Pirner, and T. Kunihiro, Phys. Rev. C **61**, 035202 (2000).
[30] J. Braun, K. Schwenzer, and H. J. Pirner, Phys. Rev. D **70**, 085016 (2004).
[31] J. Zinn-Justin, *Quantum Field Theory and Critical Phenomena* (Clarendon, Oxford, 1989), International series of monographs on Physics, vol. 77.
[32] D. U. Jungnickel and C. Wetterich, Phys. Rev. D **53**, 5142 (1996).
[33] J. Berges, D. U. Jungnickel, and C. Wetterich, Phys. Rev. D **59**, 034010 (1999).